Impact of molecular mass on the elastic modulus of thin polystyrene films ☆

Jessica M. Torres [a], Christopher M. Stafford [b], Bryan D. Vogt [a],*

[a] Flexible Display Center, Arizona State University, Tempe, AZ 85284, USA
[b] Polymers Division, National Institute of Standards and Technology, Gaithersburg, MD 20899, USA

ARTICLE INFO

ABSTRACT

Surface wrinkling was used to determine the elastic modulus at ambient temperature of polystyrene (PS) films of varying thickness and relative molecular mass (M_n). A range of M_n from 1.2 kg/mol to 990 kg/mol was examined to determine if the molecular size impacts the mechanical properties at the nanoscale. Ultrathin films exhibited a decrease in modulus for all molecular masses studied here compared to the bulk value. For $M_n > 3.2$ kg/mol, the fractional change in modulus was statistically independent of molecular mass and the modulus began to deviate from the bulk as the thickness is decreased below ≈ 50 nm. An order of magnitude decrease in the elastic modulus was found when the film thickness was ≈ 15 nm, irrespective of M_n. However, an increase in the length scale for nanoconfinement was observed as the molecular mass was decreased below this threshold. The modulus of thin PS films with a molecular mass of 1.2 kg/mol deviated from bulk behavior when the film thickness was decreased below ≈ 100 nm. This result illustrates that the modulus of thin PS films does not scale with molecular size. Rather, the quench depth into the glass appears to correlate well with the length scale at which the modulus of the films deviates from the bulk, in agreement with molecular simulations from de Pablo and coworkers [31] and recent experimental work [35].

© 2010 Elsevier Ltd. All rights reserved.

1. Introduction

The influence of confinement of polymer chains to length scales approaching their intrinsic dimensions has fascinated scientists for decades [1]. In particular, the glass transition temperature (T_g) of ultrathin polymers has been studied extensively [2,3]. The relative ease of these measurements coupled with the strong correlation of T_g on other properties of polymeric materials such as elastic modulus, loss modulus, and the coefficient of thermal expansion [4] has provided a wealth of information regarding the physical properties of thin polymer films. In particular, polystyrene (PS) has become a model system for thin film measurements [5–7], but even for this system, there are inconsistent results regarding the direction of deviations [8,9] in T_g of thin PS films and the influence of molecular mass [10,11]. Thus for predicting mechanical stability of polymeric nanostructures, more direct measurements of the mechanical properties such as Young's modulus is desired for polymers when confined to nanometer dimensions, as the relationship between mechanical properties and T_g at the nanoscale is unclear.

Additionally, the physical origins of the deviations in properties of thin polymer films are still being debated. Two potential origins have been discussed based upon (1) the confinement of the polymer chains [1,12] and (2) increased contributions from interfacial effects as the film thickness is decreased [5] (increased surface area to volume ratio). Typically the characteristic size used is the radius of gyration, R_g. At film thicknesses of several R_g, deviations in the physical properties of the polymer relative to the bulk are generally observed for a host of different properties [13–15]. Thus, molecular mass would be expected to significantly influence the behavior of thin films [12]. However, there exists growing evidence that T_g is independent of molecular mass in thin films [10,16]. Rather, the influence of substrate–polymer interactions [17,18] as well as polymer-free surface interactions [19,20] have been suggested to cause the observed changes in T_g of thin polymer films. For example, free standing PS films show a further reduction in T_g by approximately 20 °C compared to analogous PS films supported on silicon wafers [8,21]. Additionally, theory [21] and experiments [19] have illustrated a gradient in T_g that extends from the free surface. The relaxation of surface topography below bulk T_g also illustrates the enhanced mobility at the free surface of polymers [22,23]. Using random first order transition theory, Stevenson and Wolynes have shown that dynamics near the surface of glasses is much faster than in the bulk [24]. However, the mechanical properties of PS thin films have been probed with contradictory results. In one case,

---

a 200% increase in the surface stiffness occurs within 200 nm of the surface of PS as probed by nanoindentation [25]. This increased modulus is attributed to polymer densification imposed by the interfacial region between the indentation probe and the polymer surface [25]. Conversely by using an atomic force microscopy (AFM) to control the indentation depth, the top 5–7 nm of PS films has been shown to have a significantly reduced elastic modulus [26,27]. Alternatively, no apparent change in stiffness of PS for films as thin as 29 nm was observed using Brillouin light scattering (BLS), despite the large depression in T_g (60 °C) from bulk [28]. Using wrinkling, the elastic modulus of high molecular mass PS films was found to be depressed in thin films less than ≈ 40 nm thick [29]. Simulations by de Pablo and coworkers suggest the existence of a surface layer at the air–polymer interface that leads to a reduction of mechanical properties that is dependent on the quench depth $(T - T_{g,bulk})$ [30,31].

These experimental and simulation results call into question some of the common assumptions regarding the relationship between thin film T_g and mechanical properties [32,33]. Moreover, McKenna and coworkers have demonstrated that the rheological properties of thin polymer films can change in comparison to the bulk even in the absence of any change in the T_g of thin films [34]. Similarly, we have recently reported that the elastic modulus of poly(n-propyl methacrylate) thin films decreases at length scales where no change in T_g is observed [35]. These results suggest that changes in polymer T_g due to confinement is not necessarily directly correlated with the moduli of polymer thin films.

In this article, the influence of molecular mass on the moduli of polystyrene thin films is examined using a wrinkling based metrology, which has been demonstrated for film thicknesses down to 5 nm [35,36]. This metrology takes advantage of a phenomenon known as Euler-type wrinkling instability, which occurs upon compression of a soft substrate with an integrated stiff polymer film. Due to a minimization of the total strain energy, the resulting surface is comprised of sinusoidal undulations having a dominant wavelength, λ. When the substrate is much thicker than the film (semi-infinite) and the modulus of the film is much greater than the modulus of the substrate, the wavelength remains independent of strain as long as the substrate is linear elastic [37]. This strain invariance of λ results in a simple route to deduce the thin film modulus, $\overline{E}_f$, if the modulus of the substrate, $\overline{E}_s$, and the film thickness, h_f, are known. The relationship between the film modulus and the wrinkling wavelength is given by

$$\overline{E}_f = 3\overline{E}_s \left(\frac{\lambda}{2\pi h_f} \right)^3 \tag{1}$$

Previous studies for two high molecular mass $(M_n > 100$ kg/mol) PS films have showed that the thin films' moduli are not strongly dependent upon molecular mass. However, understanding if there is any dependence of the modulus on M_n for thin films is important from both a fundamental and practical prospective. For example, low M_n polystyrene nanostructures are typically formed using block copolymer lithography [38,39]; their mechanical properties are important to the ultimate stability of the nanostructures. To address this issue, a wide range of PS molecular mass from 1.2 kg/mol to 990 kg/mol is examined to determine how molecular mass impacts the elastic modulus of thin polymer films. We demonstrate that low molecular mass films exhibit a decrease in modulus at larger film thickness, which scales with quench depth into the bulk glass.

2. Experimental

Note that certain commercial equipment, instruments, or materials are identified in this document. Such identification does not imply recommendation or endorsement by the National Institute of Standards and Technology (NIST), nor does it imply that the products identified are necessarily the best available for this purpose. PS with varying molecular mass was purchased from Polymer Laboratories. The physical characteristics of these polymers are listed in Table 1. The PS used in this study is synthesized with butyllithium initiator and are methyl terminated. The molecular mass of the PS samples were independently measured by gel permeation chromatography (GPC) using a Waters Breeze 2 equipped with a Waters 1515 high-performance liquid chromatography pump and a Waters 2414 refractive index detector. Two size exclusion chromatography columns (Waters HT2 and HT6E) with tetrahydrofuran as the mobile phase were used at a flow rate of 1 mL/min to separate, identify, and quantify samples. Samples were prepared at 2 mg/mL for GPC characterization. Data processing was conducted using the GPC Isocratic Technique in the Breeze software. A 3rd order calibration was conducted using Polymer Labs Easical PS2B as the calibrant. The glass transition temperature of each PS was measured using differential scanning calorimetry (DSC), which was performed on a TA Instruments Q1000 heat flux DSC under a dry nitrogen purge (50.0 mL/min). All runs were performed at heating and cooling rates of 10 °C/min in T4P mode, and temperature calibration for heating runs was achieved using an indium standard at the same heating rate. Silicon wafers (450 μm thick) were used as substrates after being cut into 2.5 cm × 1 cm pieces and cleaned with ultraviolet/ozone (model 342, Jelight, Inc.). Dilute polymer solutions were spin-cast from toluene onto the wafers to create thin films of uniform thickness. Film thickness was controlled by PS concentration (0.2–2% by mass PS) and spin speed (150 rad/s to 265 rad/s). The thickness of the polymer film was determined using a Variable Angle Spectroscopic Ellipsometer (VASE, J.A. Woollam Co., Inc.) over a wavelength range from 250 nm to 1700 nm at three incident angles, 67°, 70°, and 73°. The data were fit using a Cauchy layer to represent optical constants of the polymer.

Polydimethylsiloxane (PDMS) (Sylgard 184, Dow Corning) was prepared at a ratio of 20:1 by mass of base to curing agent and cast on float glass to a thickness of approximately 1.5 mm. The PDMS was allowed to gel at room temperature for 3 h before curing at 100 °C for 2 h. After cooling the PDMS sheet was cut into 2.5 cm × 7.5 cm × 1.5 mm slabs. The modulus of the bulk PDMS sheets was determined using a tensile test (Instron) at a cross head speed of 0.01 mm/s along the long dimension. The PDMS was pre-strained to 3% on a custom stage [40]. The polymer film supported on the silicon wafer was placed in contact with the strained PDMS, and then immersed in water. Due to differential adhesion in water, the polymer film was transferred from the wafer onto the PDMS. The sample was allowed to dry under vacuum at 10 °C below its bulk T_g to prevent thermal wrinkling. The film thickness of some samples was then re-measured with VASE. No statistical difference in film thickness was observed after transfer. The pre-strain on the PDMS was released at a rate of 0.1 mm/s. All samples were released at ambient temperature $(T = 21$ °C ± 2 °C$)$. To minimize the compressive strain which is greater than the critical strain [29], the

Table 1
Physical characteristics of PS utilized in this study.

M_n (kg/mol)	M_w/M_n	$T_{g,bulk}$ (°C)	$\overline{E}_{bulk}$ (GPa)
990	1.05	106.3 ± 2.0	3.81 ± 0.22
492	1.03	106.1 ± 2.5	3.92 ± 0.27
9.4	1.06	94.1 ± 2.3	3.90 ± 0.21
3.2	1.05	76.1 ± 2.2	3.44 ± 0.21
2.3	1.05	62.3 ± 1.5	3.37 ± 0.26
1.3	1.13	29.9 ± 3.1	1.76 ± 0.24
1.2	1.13	21.3 ± 3.2	1.30 ± 0.17
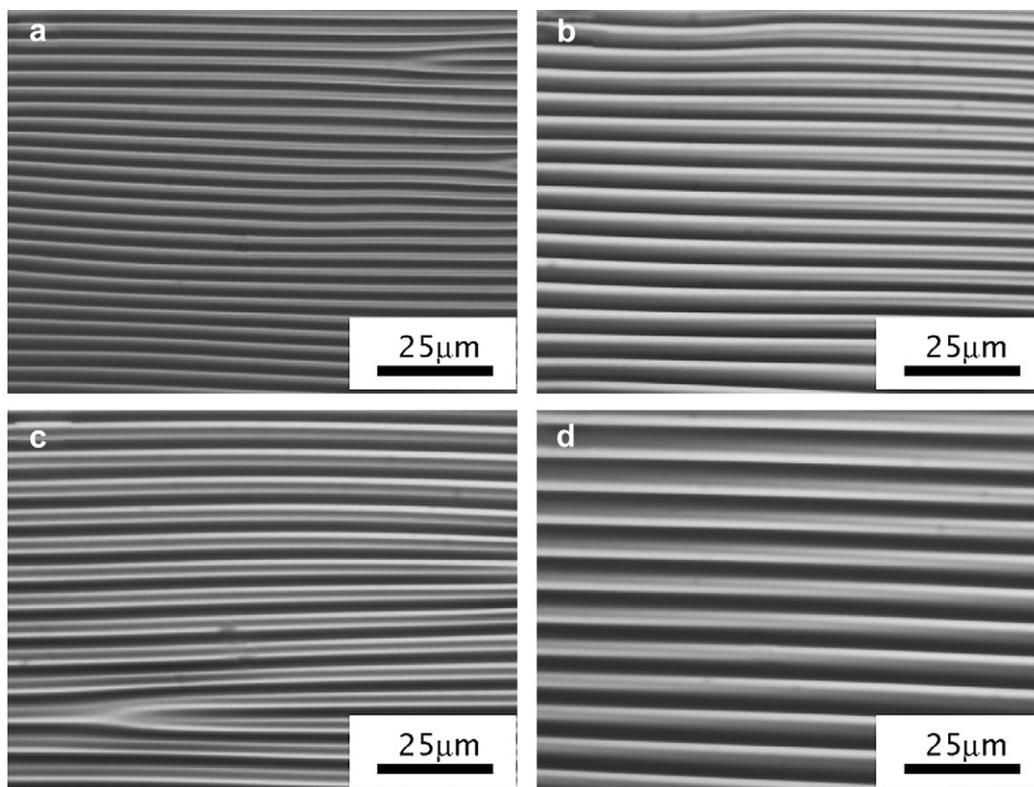
Fig. 1. Optical micrographs of wrinkled 990 kg/mol PS films that are (a) 48 nm, (b) 62 nm, (c) 81 nm, and (d) 101 nm thick. The wavelength of the wrinkles increases as the film thickness is increased.

film undergoes periodic wrinkling. It is important to note that any excess strain results only in an increase in the amplitude of the wrinkles without changing the wavelength as long as the film and substrate remain linear elastic. Furthermore, analytical expressions for the stress field and finite element analysis indicate that the modulus of the PDMS substrate is probed at depths of approximately several wavelengths. Since the wavelength is greater than 500 nm for the thinnest polymer films examined here, the interfacial mechanical properties of the PDMS should not impact the measurement, as this interfacial modulus will be averaged with the first micrometers of the bulk PDMS. For additional information regarding the relative length scales probed by the wrinkles, see supporting information in Ref. [35].
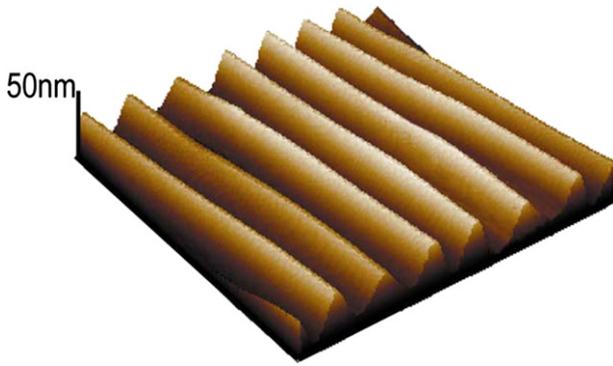
The wrinkled surfaces were characterized using AFM and optical microscopy. AFM micrographs were acquired at ambient temperature on an Agilent Technologies 5500 system in tapping mode using Pico Plus 1.0 software at constant scan size of 7.5 μm × 7.5 μm and scan speed of 1 line/s. Optical micrographs were acquired on a Mititoyo Ultraplan FS-110 with an image resolution of 768 pixels × 1024 pixels. The wrinkling wavelength was determined using 1-D fast Fourier transforms (FFT) of the micrographs.

3. Results

Fig. 1 shows optical micrographs of wrinkled 990 kg/mol PS films for a series of different film thicknesses. As the film thickness is decreased from 101 nm to 48 nm, the equilibrium wavelength decreases from 8.2 μm ± 0.41 μm to 3.4 μm ± 0.12 μm, respectively[1].

As expected from wrinkling mechanics (Eq. (1)), the wavelength depends linearly on the film thickness. For thinner films, the wrinkles cannot be resolved with optical microscopy and instead AFM is utilized. As shown in Fig. 2, the equilibrium wavelength for a 25 nm film of the 990 kg/mol PS decreases to 1.28 μm ± 0.31 μm. However, this reduction in wavelength is greater than expected unless there is also a decrease in the modulus of the film. By examining the thickness dependence of the wavelength, a more comprehensive picture of how the moduli of the PS films vary with thickness can be constructed. Fig. 3 illustrates how the wrinkle wavelength, λ, depends upon the film thickness, h_f, for a series of different molecular mass PS films where the substrate modulus, $\overline{E}_s$, is nominally constant. The wavelength shows a linear dependence upon the film thickness for all molecular masses examined, but the slope of the data begins to decrease slightly when the molecular mass is decreased below 3.2 kg/mol. The slope changes from 77.6 μm/nm for $M_n > 3.2$ kg/mol PS to 70 μm/nm for 1.3 kg/mol PS to 65 μm/nm for 1.2 kg/mol PS. This change in slope corresponds to a decrease in the bulk modulus of the films. This slope only directly correlates to the elastic modulus of the film if the PDMS modulus is constant and the film modulus does not vary significantly with film thickness. Note that T_g of PS also decreases precipitously in this molecular mass region (Table 1). It should be noted that the modulus of PS might be expected to decrease at much higher molecular mass (entanglement M_n) based upon bulk rheological properties of PS melts. However in this case, the elastic moduli of the PS glass are probed with small strain deformations. Only short length scales are probed with this measurement; for entanglements to become important larger deformations are necessary in glassy films. The length scales probed and underlying polymer physics involved in determining the elastic modulus of these glassy PS films using wrinkling differs substantially from measurements of PS film viscoelasticity [41] determined by dewetting kinetics. In

---

[1] The data throughout the manuscript and the figures are presented along with the standard uncertainty (±) involved in the measurement based on one standard deviation.

Fig. 2. AFM images of wrinkled films of 25 nm thick 990 kg/mol PS film. Scan size is 7.5 μm × 7.5 μm and the height scale of the micrograph is 50 nm as shown.

Table 2
Bilayer model fit for different molecular mass PS films with comparison of the thickness of surface layer from the bilayer model (model) and the linear extrapolation (linear) to zero wavelength.

M_n (kg/mol)	$\bar{E}_f$ (GPa)	$\bar{E}_f^*$ (GPa)	h^* (nm) (model)	h^* (nm) (linear)
990	3.81 ± 0.22	0.171 ± 0.037	5.4 ± 1	5.5 ± 0.5
492	3.92 ± 0.27	0.139 ± 0.045	5.6 ± 1.2	5.7 ± 0.5
9.4	3.90 ± 0.21	0.095 ± 0.079	5.9 ± 1.6	5.9 ± 0.3
3.2	3.44 ± 0.21	0.086 ± 0.046	7.0 ± 1.9	6.0 ± 0.7
2.3	3.37 ± 0.26	0.052 ± 0.014	10.3 ± 1.9	10.1 ± 0.1
1.3	1.76 ± 0.10	0.046 ± 0.010	27.5 ± 1.6	18.2 ± 0.1
1.2	1.30 ± 0.17	0.026 ± 0.003	59.1 ± 2.5	37.3 ± 0.2

this later experiment, large scale chain motion is required and thus the measurement is sensitive to entanglements as well as the stress state in the film. One advantage of the wrinkling method is that residual stress only impact the amplitude of the wrinkles, not the wavelength [42]. Additionally, the wavelength of the wrinkles is stable over at least the timeframe of weeks as long as bulk T_g is not exceeded. As the modulus of the film can be directly elucidated from the wavelength, residual stress and the non-equilibrium state of the spin coated film do not impact the measurement. Previous studies have shown that annealing PS films above T_g does not impact the thin film modulus determined from wrinkling [36]. This lack of sensitivity to thermal history is not entirely unexpected as the elastic modulus of PMMA deep in the glass is unchanged by annealing [43].

Another feature of the data in Fig. 3 is that the extrapolated wavelength does not extend through the origin as would be expected for films with a constant $\bar{E}_f$ and the intercept of the linear fit shifts to larger thickness as M_n is decreased below 3.2 kg/mol. Taking a cue from thin film T_g studies [8,17,19,21], this deviation in the extrapolated wavelength is likely due to interfacial effects arising from the free surface and/or the polymer–substrate interaction that lead to a reduced modulus. A trilayer model consisting of a surface layer, middle 'bulk-like' layer, and a substrate interface layer has been successfully applied to understand the thin film T_g behavior of polymer thin films [5] and a similar approach can likely be applied to thin film moduli. However for T_g of PS thin films supported on silicon oxide, selective fluorescence labeling has
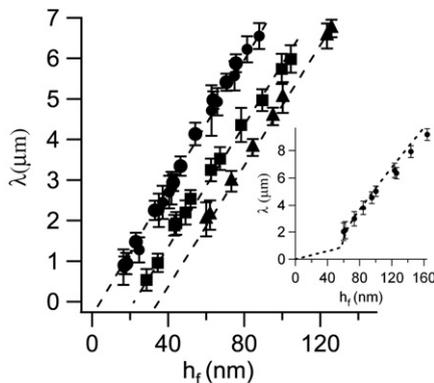
Fig. 3. Wrinkle wavelength dependence on film thickness for (●) 990 kg/mol, 492 kg/mol, 9.4 kg/mol, 3.2 kg/mol (■) 1.3 kg/mol, and (▲) 1.2 kg/mol PS. The extrapolated wavelengths intersect at thicknesses that are generally representative of surface layer of reduced modulus. The dashed lines are linear fits to the data, and the error bars represent one standard deviation of the data, which is taken as the experimental uncertainty of the measurement. (Inset) The wavelength data for the 1.2 kg/mol PS films can be fit by the bilayer model with the parameters shown in Table 2.

indicted that there is no change in T_g at the substrate interface and the free surface dominates the reduction in thin film T_g. In this case, a two-layer model consisting of bulk-like polymer with a reduced T_g surface layer is sufficient. As the interaction between most polymers and PDMS is non-attractive similar to PS and silicon oxide, the non-zero intercept has been typically attributed to a free surface layer having a reduced modulus [35,36,44]. From the linear fits of the data, the thickness of this apparent free surface layer, h^*, increases with decreasing molecular mass, from approximately 5 nm for 990 kg/mol PS to nearly 35 nm for the 1.2 kg/mol PS films as listed in Table 2. h^* is obtained from extrapolation of the data to zero λ. It is possible that the PS modulus near the PDMS is also reduced as the interaction between PS and PDMS is moderately unfavorable. In this case, h^* would represent the aggregate of the thickness of the surface and interfacial layers with reduced moduli. h^* is significantly larger than the free surface layer that has been reported for any other polymer in the literature [35,36]. A null wavelength does not mean that the modulus of this surface layer is zero, but rather that the critical strain (which depends upon the ratio of the film to PDMS modulus) has not been exceeded [29]. As the bulk T_g of the polymer is decreased (due to the decrease in M_n), h^* increases for a fixed measurement temperature, in this case 21 °C ± 2 °C. The increase in the length scale at which a deviation in modulus occurs with decreasing quench depth agrees with predictions from de Pablo and coworkers [30,31]. The length scale for the deviation in bulk modulus actually increases as R_g decreases; this result strongly suggests that the change in mechanical properties of thin polymer films is due to increased interfacial (free surface) effects, rather than being an intrinsic effect from confinement of the polymer chains.

Using Eq. (1), the wavelength data can be used to quantify the modulus of the PS thin films as shown in Fig. 4. The data in Fig. 4 show a similar pattern for each molecular mass PS. For thicker films, the modulus is essentially independent of thickness. However once a critical film thickness is reached, the modulus decreases significantly from the bulk value. From Eq. (1), it is also possible to interpret this change in wavelength as a result of changes in the elastic properties of the PDMS. However, the probe depth into the PDMS during the surface wrinkling is a multiple of λ; thus, the top micron of the PDMS must behave significantly stiffer (order of magnitude) than the bulk in order to account for the observed wrinkle wavelength if the modulus of the PS is unaffected by film thickness. However, nanoindentation measurements of PDMS yield moduli similar to those obtained by DMA and show no indications of a stiff surface layer [45]. Furthermore, the base to cure ratio in the PDMS has been varied from 10:1 to 20:1 and the calculated moduli of the PS films is independent of the cure ratio. It is highly unlikely that the surface modulus of PDMS is independent of base to cure ratio; moreover, the film thickness at which deviations in the wavelength occur is dependent upon the polymer as shown in Fig. 4. These results indicate that the surface properties of PDMS are not responsible for the deviations in the wrinkle
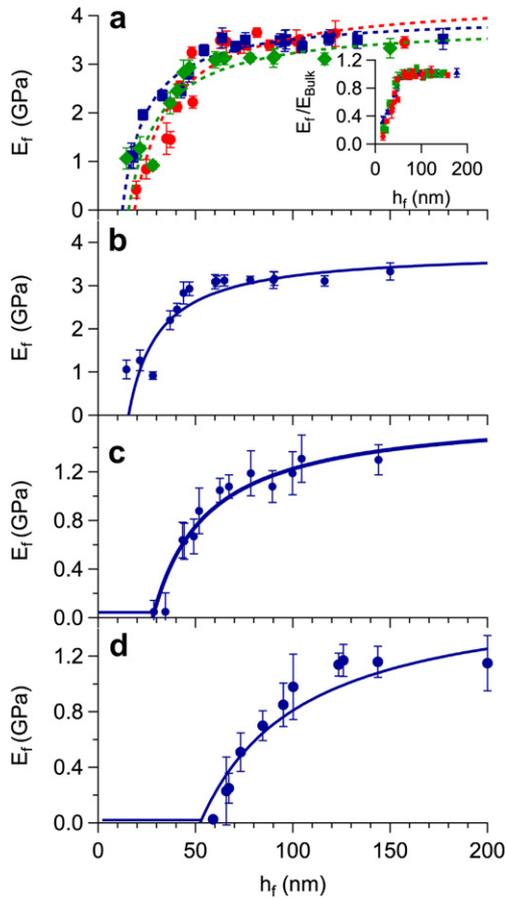
Fig. 4. Film thickness dependence of the modulus of PS thin films for molecular masses of (a) 990 kg/mol (●, red), 9.4 kg/mol (■, blue), and 3.2 kg/mol (◆, green), (b) 2.3 kg/mol, (c) 1.3 kg/mol, and (d) 1.2 kg/mol. The inset in (a) illustrates the collapse of the reduced elastic modulus for a wide range of molecular masses down to 3.2 kg/mol. The solid lines are bilayer model fits to the data. The error bars represent one standard deviation of the data, which is taken as the experimental uncertainty of the measurement. (For interpretation of the references to colour in this figure legend, the reader is referred to the web version of this article.)

wavelength observed here, instead we attribute the variable mechanical properties to film thickness dependent elastic properties of PS.

For PS films with $M_n > 3.2$ kg/mol, the reduced modulus ($E_s/E_{f,\,bulk}$) as a function of film thickness collapses onto a single curve, as shown in the inset to Fig. 4a. The thickness at which this observed deviation in elastic modulus occurs is ≈ 50 nm, which is consistent with prior reports for high molecular mass PS [36]. Additionally, simulations suggest a length scale of ≈ 40 nm for deviations in mechanical properties when the polymer is quenched deep into the glass [30,31]. For M_n of 3.2 kg/mol and 2.3 kg/mol, the thick film ("bulk") modulus is reduced relative to the higher M_n PS films by approximately 10%. The thickness at which the deviation from bulk behavior is observed is not greatly affected and still occurs at ≈ 50 nm. However, a further decrease in M_n to 1.3 kg/mol results in a significant decrease in the bulk modulus as well as a shift in the critical thickness to nearly 70 nm. In this case, the

quench depth into the bulk glass is less than 10 °C. Simulations have suggested that near bulk T_g the mechanical properties of polymer thin films will begin to deviate from the bulk at approximately 80 nm [30,31]. The experimental results reported here are in good agreement with those simulations. Interestingly, when the quench depth into the glass is ≈ 1 °C (i.e., 1.2 kg/mol PS) the polymer films begin to exhibit deviations from bulk modulus values at approximately 100 nm. This length scale is extremely large for observing nanoconfinement effects, although even longer length scales for T_g deviations have been reported [10]. It is important to note when the temperature is increased above T_g for this low M_n PS the wrinkles begin to disappear, but without any change in wrinkle wavelength. Further, the wrinkle wavelength is found to be stable over the course of days (as long as $T < T_g$). Irrespective, it is compelling that deviation in modulus at long length scales occurs for such a small M_n PS. Thus, it appears that the quench depth into the bulk glass ($T_{g,\,bulk} - T$) is a key parameter for determining the elastic moduli behavior of thin glassy films.

To better assess the surface layer effect, a bilayer model has been proposed and used in the past [44]. In this model, the polymer film consists of two distinct layers: a surface layer of thickness h^* and elastic modulus $\overline{E}_f^*$, and the remainder of the film of thickness $h_f - h^*$ and bulk elastic modulus $\overline{E}_f$; this model is used to extract the relative size of a soft surface layer based upon the *average film modulus* that can be directly assessed by application of mechanics (Eq. (1)) to the wavelength data (Fig. 3). The moduli reported in Fig. 3 are not dependent upon this bilayer model, but this model can provide an estimate for the thickness of the soft surface of PS that has been predicted [30,31] and observed experimentally [5,17,19,22,23,27]. Additionally, h^* is assumed to be a material property and independent of h_f. One potential shortcoming of this model is that it neglects the polymer–substrate interaction, which can be dominant for thin film T_g in the case of attractive surfaces [2]. For this bilayer model, the film elastic modulus is then a function of both the bulk $\overline{E}_f$ and the surface elastic modulus ($\overline{E}_f^*$) (both are material properties and independent of film thickness) as [44]:

$$\overline{E}_{f,\,\text{Stretching}} = \overline{E}_f\left(1 - \frac{h^*}{h_f}\right) + \overline{E}_f^*\left(\frac{h^*}{h_f}\right) \tag{2}$$

This bilayer simplification provides a model with a minimal number of fitting parameters, where the thickness of the free surface layer, h^*, the bulk modulus, $\overline{E}_f$, and the reduced modulus of the free surface, $\overline{E}_f^*$, are fit using Eq. (3) which accounts for both stretching and bending modulus.

$$\lambda = 2\pi h_f \left(\frac{\overline{E}_f\left(1 - \frac{h^*}{h_f}\right)^3 + \overline{E}_f^*\left(\frac{h^*}{h_f}\right)^3 + 3\overline{E}_f\left(1 - \frac{h^*}{h_f}\right)\left(1 - \xi - \frac{h^*}{h_f}\right)^2 + 3\overline{E}_f^*\left(\frac{h^*}{h_f}\right)\left(2 - \xi - \frac{h^*}{h_f}\right)^2}{3\overline{E}_s}\right)^{1/3} \tag{3}$$

where

$$\xi = \frac{\overline{E}_f\left(1 - \frac{h^*}{h_f}\right) + \overline{E}_f^*\left(\frac{h^*}{h_f}\right)\left(2 - \frac{h^*}{h_f}\right)}{\overline{E}_f\left(1 - \frac{h^*}{h_f}\right) + \overline{E}_f^*\left(\frac{h^*}{h_f}\right)} \tag{4}$$

It should be noted that there is likely a distribution of moduli through the film thickness, similar to the distribution of T_gs observed in thin films [19]. However, this bilayer model has been shown to fit the experimentally obtained elastic moduli of thin films of high molecular mass polystyrene and poly(methyl methacrylate) [36] and as such has been applied here to provide an

estimate of the surface effect as a function of molecular mass. The fits to the bilayer model are shown by the dashed lines in Fig. 4. Table 2 lists the thickness of the free surface layer as well as the apparent modulus of both the free surface layer and the bulk layer as a function of molecular mass that is obtained from the fits. The free surface layer maintains a near constant thickness of approximately 5.7 nm and plane-strain modulus of ≈ 0.1 GPa for >3.2 kg/mol PS. As the molecular mass decreases below 3 kg/mol, the free surface layer thickness (h^*) increases significantly. For high molecular masses, the h^* from the bilayer fits corresponds well with the h^* (intercept) obtained from linear fits of the wavelength data, as shown in Table 2. However, the dependence of h^* on wavelength is non-linear [44]. While the curvature is small, this leads to underestimation of the thickness of the soft surface layer. As the thickness of the layer increases, the disagreement with the extrapolated estimate increases. For example, there is disagreement in h^* for $M_n = 1.2$ kg/mol between the two methods, with h^* from the fit and the extrapolation differing by a factor of 2 with a smaller value from the extrapolation. The linear extrapolation is only an approximation, but it provides an accurate estimate at $h^* < 15$ nm as shown previously [29,35]. The solid line in the inset of Fig. 3 illustrates the excellent fit of the wavelength data by the bilayer model using $h^* = 59.1$ nm. Due to the potential inaccuracies associated with the extrapolated thickness for large h^*, the surface layer thickness obtained from the bilayer fit will be utilized for additional analyses as it provides a better physical model for the changes in wavelength. In addition to the changes in h^* with M_n, the critical thickness where deviations in modulus from the bulk value occur increases to larger thickness.

The increase in critical thickness with decreasing M_n for the low molecular mass PS suggest the quench depth ($T - T_{g,bulk}$), rather than finite chain confinement based upon molecular size, is a key parameter in determining the mechanical behavior of polymer thin films. Fig. 5 illustrates the dependency of quench depth on the length scales where deviations in the elastic modulus of thin PS films occurs, as revealed by h^* determined from the bilayer fit. For comparison, the dependence of h^* on quench depth for a series of poly(n-alkyl methacrylate)s reported previously [35] are also included in Fig. 5. Interestingly, these data quantitatively agree with PS here. The interactions between PDMS and these polymers are not identical, so
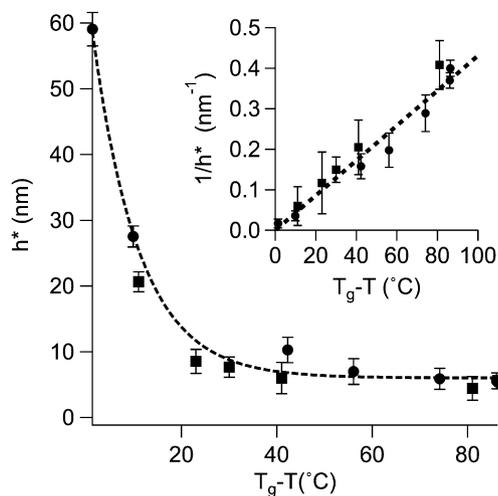
it is unlikely that the PDMS–polymer interface significantly impacts the thin film moduli for these polymer films based upon the agreement in h^* shown in Fig. 5. Thus, we have utilized the simple bilayer model in the analysis of the moduli data. At relatively large quench depths for the PS, the surface layer thickness is essentially constant at approximately 5 nm. This result suggests that there is a nearly constant thickness soft surface layer for high M_n PS films. This thickness is consistent with prior reports in the literature regarding a soft surface layer that is approximately 5 nm thick [46–48]. As M_n and $T_{g,bulk}$ decrease, the thickness of the surface layer increases dramatically. h^* appears to diverge near T_g. At T_g, it would be expected that the entire film irrespective of thickness would have a low modulus, which would be similar to the bulk modulus of the rubber. It should be noted that T_g is rate dependent and thus the T_g determined by DSC and the T_g of the polymer in regards to wrinkle formation (rate of strain release) may be slightly different. As shown in Fig. 5, h^* increases rapidly as T_g (DSC) is approached. This dependency of the apparent surface layer thickness, as determined from our modulus measurements, on the proximity of the bulk T_g may lend insight into glass formation in polymers where the near surface remains more mobile (lower modulus) than the bulk. The expansion of the rubbery-like surface layer as the bulk T_g is approached is reminiscent of the growth of the liquid phase from the free interface into glassy tris-naphthylbenzene [49]. The surface layer dependence on quench depth can be fit equally well by an exponential and inverse (inset) relationship as shown in Fig. 5. Simulations have suggested that fast segmental motions [50–52] near the free surface initiate cooperative motion of many segments and results in an enhanced polymer mobility [53] that leads to a decrease in modulus [30,31]. However, additional theoretical work on the relationship between quench depth and the modulus of nanoconfined polymers is required to understand exactly how the soft surface thickness scales. Nonetheless, the surface layer thickness appears to be well correlated with the quench depth into the bulk glass for all molecular masses of PS examined here.

4. Conclusion

The elastic modulus of ultrathin films for a series of varying molecular mass (1.2 kg/mol < M_n < 990 kg/mol) polystyrene films has been elucidated using surface wrinkling of a stiff polymeric film on an elastic substrate. As expected, the modulus of the bulk of the film decreases as M_n decreases below a threshold (≈ 3.2 kg/mol). However, a decrease in the modulus of the thin films with respect to the invariant thick film modulus is found for all M_n PS examined. The modulus deviation from bulk values is attributed to a free surface effect at the polymer/air interface. For high M_n (>3.2 kg/mol), the deviation in modulus is independent of molecular mass and begins when the film thickness is less than ≈ 50 nm. However at $M_n = 1.2$ kg/mol, the modulus decreases at much larger thickness (≈ 100 nm). This change in the length scales is directly related to the layer thickness of the lower modulus surface. The thickness of the soft surface layer determined from a bilayer model varies from ≈ 5 nm deep in the glass to greater than 50 nm when the measurement occurs within ≈ 1 °C of $T_{g,bulk}$. The deviation in the modulus of thin films appears to scale directly with the quench depth into the bulk glass.

Fig. 5. Free surface layer thickness as determined from the bilayer model is strongly correlated with quench depth into the glass for (●) PS and (■) poly(n-alkyl methacrylate)s. The data for the polymethacrylates are taken from [35]. The dashed lines are exponential and linear (inset) fits of the data, and the error bars represent one standard deviation of the data, which is taken as the experimental uncertainty of the measurement.

References

[1] Forrest JA, Dalnoki-Veress K. Adv Colloid Interfac Sci 2001;94:167–96.
[2] Fryer DS, Peters RD, Kim EJ, Tomaszewski JE, de Pablo JJ, Nealey PF, et al. Macromolecules 2001;34:5627–34.
[3] McKenna GB. J Phys IV 2000;10:53–7.
[4] Ngai KL, Plazek DJ. Rubber Chem Technol 1995;68:376–434.
[5] DeMaggio GB, Frieze WE, Gidley DW, Zhu M, Hristov HA, Yee AF. Phys Rev Lett 1997;78:1524–7.
[6] Fukao K, Miyamoto Y. Phys Rev E 2000;61:1743–54.
[7] Kanaya T, Miyazaki T, Watanabe H, Nishida K, Yamana H, Tasaki S, et al. Polymer 2003;44:3769–73.
[8] Forrest JA, DalnokiVeress K, Dutcher JR. Phys Rev E 1997;56:5705–16.
[9] Huth H, Minakov AA, Serghei A, Kremer F, Schick C. Eur Phys J 2007; 141:153–60.
[10] Ellison CJ, Mundra MK, Torkelson JM. Macromolecules 2005;38:1767–78.
[11] Singh L, Ludovice PJ, Henderson CL. Thin Solid Films 2004;449:231–41.
[12] Forrest JA, Mattsson J. Phys Rev E 2000;61:R53–6.
[13] Lin EK, Wu WI, Satija SK. Macromolecules 1997;30:7224–31.
[14] Shin K, Obukhov S, Chen JT, Huh J, Hwang Y, Mok S, et al. Nat Mater 2007;6:961–5.
[15] Soles CL, Douglas JF, Jones RL, Wu WL. Macromolecules 2004;37:2901–8.
[16] Seemann R, Jacobs K, Landfester K, Herminghaus S. J Polym Sci B 2006; 44:2968–79.
[17] Keddie JL, Jones RAL, Cory RA. Faraday Discuss 1994;98:219–30.
[18] vanZanten JH, Wallace WE, Wu WL. Phys Rev E 1996;53:R2053–6.
[19] Ellison CJ, Torkelson JM. Nat Mater 2003;2:695–700.
[20] Priestley RD, Ellison CJ, Broadbelt LJ, Torkelson JM. Science 2005;309:456–9.
[21] de Gennes PG. Eur Phys J E 2000;2:201–3.
[22] Fakhraai Z, Forrest JA. Science 2008;319:600–4.
[23] Knoll A, Wiesmann D, Gotsmann B, Duerig U. Phys Rev Lett 2009;102:117801.
[24] Stevenson JD, Wolynes PG. J Chem Phys 2008;129:234514.
[25] Tweedie CA, Constantinides G, Lehman KE, Brill DJ, Blackman GS, van Vliet KJ. Adv Mater 2007;19:2540–6.
[26] Meyers GF, Dekoven BM, Seitz JT. Langmuir 1992;8:2330–5.
[27] Miyake K, Satomi N, Sasaki S. Appl Phys Lett 2006;89:4365–7.
[28] Forrest JA, Dalnoki-Veress K, Dutcher JR. Phys Rev E 1998;58:6109–14.
[29] Stafford CM, Harrison C, Beers KL, Karim A, Amis EJ, Vanlandingham MR, et al. Nat Mater 2004;3:545–50.
[30] Bohme TR, de Pablo JJ. J Chem Phys 2002;116:9939–51.
[31] Yoshimoto K, Jain TS, Nealey PF, de Pablo JJ. J Chem Phys 2005; 122:144712.
[32] Cappella B, Kaliappan SK, Sturm H. Macromolecules 2005;38:1874–81.
[33] Mackay ME, Dao TT, Tuteja A, Ho DL, Van Horn B, Kim HC, et al. Nat Mater 2003;2:762–6.
[34] O'Connell PA, McKenna GB. Science 2005;307:1760–3.
[35] Torres JM, Stafford CM, Vogt BD. ACS Nano 2009;3:2677.
[36] Stafford CM, Vogt BD, Harrison C, Julthongpiput D, Huang R. Macromolecules 2006;39:5095–9.
[37] Duan HL, Wang J, Huang ZP, Karihaloo BL. J Mech Phys Solids 2005; 53:1574–96.
[38] Park M, Harrison C, Chaikin PM, Register RA, Adamson DH. Science 1997; 276:1401–4.
[39] Thurn-Albrecht T, Schotter J, Kastle CA, Emley N, Shibauchi T, Krusin-Elbaum L, et al. Science 2000;290:2126–9.
[40] Stafford CM, Guo S, Harrison C, Chiang MYM. Rev Sci Instrum 2005;76:062207.
[41] Bodiguel H, Fretigny C. Macromolecules 2007;40:7291–8.
[42] Chung JY, Chastek TQ, Masolka MJ, Ro HW, Stafford CM. ACS Nano 2009;3:844–52.
[43] Bodiguel H, Lequeux F, Montes H. J Stat Mech Theory Exp 2008;1:P01020.
[44] Huang R, Stafford CM, Vogt BD. J Aerospace Eng 2007;20:38–44.
[45] White CC, Vanlandingham MR, Drzal PL, Chang NK, Chang SH. J Polym Sci B 2005;43:1812–24.
[46] Fischer H. Macromolecules 2002;35:3592–5.
[47] Keddie JL, Jones RAL, Cory RA. Europhys Lett 1994;27:59–64.
[48] Sasaki T, Shimizu A, Mourey TH, Thurau CT, Ediger MD. J Chem Phys 2003; 119:8730–5.
[49] Swallen SF, Traynor K, McMahon RJ, Ediger MD, Mates TE. Phys Rev Lett 2009; 102:065503.
[50] Jain TS, de Pablo JJ. Phys Rev Lett 2004;92:155505.
[51] Mansfield KF, Theodorou DN. Macromolecules 1991;24:6283–94.
[52] Tseng KC, Turro NJ, Durning CJ. Phys Rev E 2000;61:1800–11.
[53] Jain TS, de Pablo JJ. J Chem Phys 2004;120:9371–5.